

Disorder-induced finite center-of-mass momentum Cooper pairing and its consequences to the critical temperature and superconducting gap of overdoped cuprates

Victor Velasco¹ and Marcello B. Silva Neto¹

¹*Instituto de Física, Universidade Federal do Rio de Janeiro, Caixa Postal 68528, Rio de Janeiro, Brazil*

One of the most studied classes of unconventional high-temperature superconductors is the hole-doped cuprates, where special attention is given to those doped with extra interstitial oxygens. In this context, the formation of spatially inhomogeneous agglomerates of dopant oxygen atoms in the form of nanosized puddles is not only relevant, but also subject of intense recent experimental and theoretical surveys. Following these efforts, in this work we show the consequences of the presence of networks of oxygen puddles in the superconducting state of overdoped cuprates. Starting from the inhomogeneous disordered background brought by the network of puddles, we show that an effective interaction between electrons can be mediated by the local vibrational degrees of freedom of each puddle, but the pairs arising from this interaction have a finite center-of-mass momentum \mathbf{p} , thus breaking up the Cooper channel. Furthermore, we derive an analytical expression for the amplitude of the superconducting gap $\Delta_{\mathbf{k}}$ in terms of disorder and finite center-of-mass momentum and show that amplitude fluctuations are induced in the superconducting state by the presence of the puddles, where both the gap and the critical temperature are affected and reduced by disorder and finite momentum pairs. Finally, we discuss our findings in the context of networks of superconducting oxygen nano-puddles in cuprates.

I. INTRODUCTION

It is a well known fact within the Bardeen-Cooper-Schrieffer (BCS) theory of superconductivity that the two quasi-particles forming the bound states that constitute the superconductor, named Cooper pairs, have momentum k and $-k$, near the Fermi surface, with opposite spins \uparrow and \downarrow , forming a singlet with zero center-of-mass momentum [1], in what is usually called the Cooper channel. However, the existence of a finite-momentum superconducting ground state has recently been raised theoretically [2–7] and supported by several experiments in correlated quantum materials [8–11]. Moreover, the possibility of emergent finite-momentum pair states, in the form of pair density waves, in a variety of well-established superconducting compounds, for example transition-metal dichalcogenides and in cuprates [12], points to the importance of understanding the intrinsic characteristics of these states and its interplay with other common features present in these systems, such as disorder [13] and in the presence of magnetic fields [14].

Although condensed matter models usually start from the notion of a perfect crystal, a plethora of notable effects are only accessible when this notion is no longer true. One famous example is the problem of the high- T_c superconductivity on cuprates, in which a region of d -wave pairing occurs in the form of a dome-shaped area and as a function of doping in its phase diagram. Here, doping, either intentional or accidental, usually takes place, for example, via chemical substitution in $\text{La}_{2-x}\text{Sr}_x\text{CuO}_4$ [15], or via inclusion of interstitial dopant oxygen atoms (Oi) in $\text{Bi}_2\text{Sr}_2\text{CaCu}_2\text{O}_{8+\delta}$ [16], $\text{La}_2\text{CuO}_{4+y}$ [17] or $\text{YBa}_2\text{Cu}_3\text{O}_{6.5+y}$ [18], which can be treated as point-like scattering centers as well as extended defects that introduce disorder and deviate the neighboring atoms from their crystallographic positions. This brings to light a fundamental question regarding the context of the dome-shaped area of high temperature superconductivity in cuprates, on what mechanism is responsible for the reduction in T_c upon overdoping as well as to the subsequent disappearance of super-

conductivity at a critical doping. Usually, this is ascribed to intrinsic effects, in which pairing correlations diminish with doping, due to screening of local Coulomb interactions [19], but some authors have also addressed the role of disorder in suppressing superconductivity [20–22]. Disorder, however, is usually incorporated as random on-site energies in Hubbard-like models that can lead to Anderson localization phenomena [23–25], thus it is important to extend this effects to include also the possibility of severe structural disorder within finite regions of the crystal.

One of the most significant results from the study of disorder effects in superconductivity is the well known Anderson's theorem, which states that both the transition temperature, T_c , and the isotropic gap, Δ_0 , of s -wave superconductors are insensitive to the presence of weak disorder at the mean-field level of BCS-like models [26–28]. One of the requirements of the theorem is that the density of states remains unchanged when compared to the pure metal case. As such, if the influence of disorder is strong enough to deplete the density of states, the theorem no longer holds, and disorder dramatically affects superconductivity [29]. In this case of strong disorder and high concentration of impurity centers, the superconducting correlation length is comparable to the disorder correlation length, and the mean-field equations can lead to self-organized granularity where fluctuations of the local order parameter are present [30]. This is likely to be the case for overdoped cuprate superconductors with high concentration of interstitial oxygens that can lead to the formation of nanosized oxygen puddles, regions with agglomeration of Oi, that support superconductivity [17, 18, 31–33].

The case of *unconventional* high temperature d -wave superconductivity in hole-doped cuprates is of experimental and theoretical relevance since its discovery [34]. Apart from several different physical characteristics, one of the main differences between these materials and the *conventional* BCS superconductors is that the superconducting gap amplitude is not homogenous when the system undergoes the superconducting transition. This is evidenced by scanning tunneling microscopy (STM) spectra in $\text{Bi}_2\text{Sr}_2\text{CaCu}_2\text{O}_{8+\delta}$ at different

doping levels, where the inhomogeneous gap in the superconducting regime is revealed to be represented by a variety of gap sizes and amplitudes occurring in all samples as the concentration of dopants is varied [16]. Most remarkably, there is a clear correlation between the position of Oi agglomerates and the amplitudes of the gaps, since regions with larger groups of dopants are observed to correspond to regions of larger gap amplitudes [16]. Paralelly, Oi dopants have been observed to self-organize into nanosize regions, or *puddles*, as mentioned above, via μ XRS in $\text{HgBa}_2\text{CuO}_{4+\delta}$ [35], as well as in other cuprate compounds [36]. Remarkably, it has been observed that spatial variations in the self-organization of the nanosized Oi-rich puddles have a direct effect on superconductivity, through variations in the critical temperature [37]. Therefore, it is of paramount importance a deeper understanding, from a theoretical perspective, of the role of the oxygen puddles in the physics of hole-doped cuprates.

In this work, we aim to investigate the effects of how structural disorder caused by the agglomeration of Oi in puddles is responsible for the appearance of finite (nonzero) center-of-mass (CM) momentum Cooper pairs in overdoped cuprates. This will be done by making use of a previously reported model proposed to describe how superconductivity rises in cuprates, on the underdoped side of the phase diagram, in terms of the phase synchronization of networks of nanosized superconducting puddles, rich in interstitial dopant oxygens [38]. Following, we extend the puddle model to derive analytical expressions showing how the superconducting gap, and thus the critical temperature, are affected by the presence of Cooper pairs with finite CM momentum and structural disorder. Finally, we show numerically that both T_c and Δ_0 decrease with increasing disorder, thus pointing to a simple physical mechanism to explain the closing of the superconducting dome-shaped area of the phase diagram, as being due to the reduction of the available phase space for Cooper pairing due to the development of a nonzero, finite CM momentum Cooper pairs.

This paper is divided as following: in Sec. II we explain the puddle model, which is the base for the calculations presented in this work, and derive the effective interaction between electrons and the network of puddles, giving rise to a finite CM momentum pair state. Following, in Sec. III we describe the effects of structural disorder that the agglomeration of Oi within each puddle causes to the system. In Sec. IV we derive the self-consistent equation for the amplitude of the superconducting gap in terms of disorder and finite CM momentum Cooper pairs. Then Sec. V is devoted to the numerical calculations. Finally, we discuss the implications of our results within the framework of networks of nano-sized puddles and summarize our findings in Sec. VI.

II. INHOMOGENEOUS OXYGEN PUDDLES

The oxygen rich nanopuddles have different elastic properties than their surroundings, and can therefore be considered as elastic insertions in an otherwise homogeneous medium, with its own vibrational mode, forming a network of super-

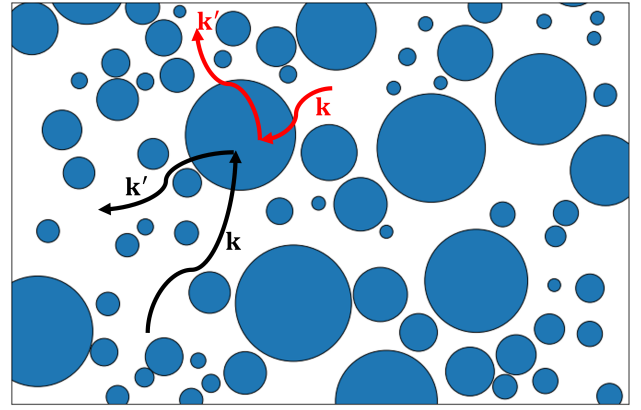


Figure 1. Pictorial view of the disordered background introduced by the network of puddles (blue) in the system. The network consists of puddles of different sizes, defined by the radius of each insertion. Electrons (black and red) scatter in each puddle and, in the superconducting state, percolate within the network.

conducting nanoscale puddles, as shown in Fig. 1, which is the starting point for the model that captured how superconductivity may arise in cuprates due to the phase synchronization of each nanopuddle [38]. In terms of the Kuramoto model for synchronization of phase oscillators [39, 40], each nanosized puddle is assigned to a phase, that in the underdoped regime evolves independently of the others, giving rise to localized patches of superconductivity, as revealed by STM and other techniques. With increased concentration of Oi through doping, the superfluid density is responsible for the enhancement of the interactions between the puddles and, in terms of the Kuramoto model, to lock their phases in a synchronous way. Following a BCS-like procedure, the order parameter for synchronization is connected to the amplitude of the bulk superconductor gap, that is non zero only after the locking of the global phase in the synchronized phase. The synchronization and the large frequency of the global network of puddles is also responsible for large values of T_c in the optimally doped cuprates within the model.

Inspired by these experimental and theoretical findings, we introduce a model Hamiltonian that captures the interaction between electrons and localized vibrations that arise from the agglomeration of interstitial oxygens in one puddle. This interaction must be local, since each electron will only interact with the quantized vibration whenever it is in the region defined by the puddle (see Fig. 1). The minimal model that captures this physical situation can be divided in $H = H_{el} + H_p + H_{el-p}$, with

$$H_{el} = \sum_{\mathbf{k}, \sigma} \xi_{\mathbf{k}} c_{\mathbf{k}, \sigma}^\dagger c_{\mathbf{k}, \sigma} + \sum_{\mathbf{k}, \mathbf{k}'} \mathcal{T}_{\mathbf{k}, \mathbf{k}'} c_{\mathbf{k}', \sigma}^\dagger c_{\mathbf{k}, \sigma},$$

where the first term represents a band of electrons with dispersion $\xi_{\mathbf{k}}$ measured relative to the chemical potential, with creation $c_{\mathbf{k}, \sigma}^\dagger$ and annihilation $c_{\mathbf{k}, \sigma}$ fermionic operators. The second term represents the scattering of electrons in each in-

homogeneity described by the puddles, with strenght controlled by the spin-preserving momentum transfer disorder matrix $\mathcal{T}_{\mathbf{k},\mathbf{k}'}$. The oxygen puddles are described by local phonon modes

$$H_p = \sum_{\mathbf{q}} \hbar \omega_{\mathbf{q}} a_{\mathbf{q}}^{\dagger} a_{\mathbf{q}},$$

with frequencies $\omega_{\mathbf{q}}$ and the creation ($a_{\mathbf{q}}^{\dagger}$) and annihilation ($a_{\mathbf{q}}$) bosonic operators, responsible for the description of the localized vibration of each puddle. Finally, the interaction term can be described as

$$H_{el-p} = \sum_{\mathbf{r}, \mathbf{R}, \sigma} g(\mathbf{r} - \mathbf{R}) c_{\mathbf{r}, \sigma}^{\dagger} c_{\mathbf{r}, \sigma} (a_{\mathbf{R}}^{\dagger} + a_{\mathbf{R}}),$$

where \mathbf{r} and \mathbf{R} are the electron and puddle locations, respectively. The puddle is a finite size region in space, thus \mathbf{R} defines the center of this region that can be modeled as a sphere. The interaction strenght $g(\mathbf{r} - \mathbf{R})$ is only relevant whenever the electron is in the region around the puddle, which can be modeled using a Gogny-type short range interaction that is dependent on the radius of the oxygen agglomeration region [41]. After performing the transformation to momentum space, the interaction term is written as

$$H_{el-p} = \sum_{\mathbf{k}, \mathbf{k}', \sigma, \mathbf{q}} M(\mathbf{q}, \mathbf{k} - \mathbf{k}') c_{\mathbf{k}, \sigma}^{\dagger} c_{\mathbf{k}', \sigma} (a_{-\mathbf{q}}^{\dagger} + a_{\mathbf{q}}), \quad (1)$$

where

$$M(\mathbf{q}, \mathbf{k} - \mathbf{k}') = \sum_{\mathbf{R}} g(\mathbf{k} - \mathbf{k}') \exp[i(\mathbf{q} - [\mathbf{k} - \mathbf{k}']) \cdot \mathbf{R}]$$

is associated with the fact that the puddles are not present in all sites, rather they are inhomogeneously distributed around the system, thus the summation has to be retained only to these regions, which is relevant for the case of $\text{Bi}_2\text{Sr}_2\text{CaCu}_2\text{O}_{8+\delta}$, since locations of dopant oxygens are observed to be consistent with the position inferred from local strain analysis of the incommensurate structure, as imaged by scanning transmission electron microscopy (STEM) [42], which means that the crucial oxygen dopants are periodically distributed in correlation with local strain. However, not all strained regions are occupied with dopant oxygen atoms, that is the distribution of Oi is inhomogeneous, which justifies our approximation and is consistent with STM measurements [43]. In the limits of a clean or a totally doped system, this term can be treated exactly. The factor $g(\mathbf{k} - \mathbf{k}')$ is the Fourier transform of the interacting potential between the electrons and the puddles and controls the momentum transfer between the incoming and scattered electron.

One can see from Eq. (1) that the presence of a finite density of puddles spread around the systems give rise to a off-diagonal term associated with the momentum transfer $\mathbf{k} - \mathbf{k}'$ that comes from the interacting potential. In the limit that the summation over $M(\mathbf{q}, \mathbf{k} - \mathbf{k}')$ can be made exactly, one recovers the usual definition of an electron-phonon interaction,

where the momentum transfer is the momentum of the local phononic mode \mathbf{q} , as in the Frohlich [44] and Holstein [45] models, for example. In order to explore the effects of this kind of interaction in the form of pairing, we introduce an unitary transformation $H' = e^{-S} H e^S$, with an *ansatz* for the transformation matrix

$$S = \sum_{\mathbf{k}, \mathbf{k}', \sigma, \mathbf{q}, \mathbf{Q}} M(\mathbf{q}, \mathbf{k} - \mathbf{k}') c_{\mathbf{k}, \sigma}^{\dagger} c_{\mathbf{k}', \sigma} (x a_{-\mathbf{q}}^{\dagger} + y a_{\mathbf{q}}),$$

where x and y are factors determined *a posteriori*. After the transformation (see Appendix A for details), we end with an effective interaction written as

$$H_{\text{eff}} = \sum_{\mathbf{k}, \mathbf{k}'} \sum_{\mathbf{p}, \mathbf{p}'} V(\mathbf{k}, \mathbf{k}') f(\mathbf{p}, \mathbf{p}') c_{\mathbf{k}, \uparrow}^{\dagger} c_{\mathbf{p}-\mathbf{k}, \downarrow}^{\dagger} c_{\mathbf{p}'-\mathbf{k}', \downarrow} c_{\mathbf{k}', \uparrow} \quad (2)$$

with $V(\mathbf{k}, \mathbf{k}') = D(\mathbf{k}, \mathbf{k}') |g(\mathbf{k} - \mathbf{k}')|^2$ being the potential arising from the interaction between electrons and puddles, $D(\mathbf{k}, \mathbf{k}')$ the phononic propagator associated with the local phonon modes produced by the vibrating puddles and $f(\mathbf{p}, \mathbf{p}') = \sum_{\mathbf{R}} e^{-i(\mathbf{p}-\mathbf{p}') \cdot \mathbf{R}}$ the phase factor controlling momentum transfer between the interacting electrons. In the regime where the phononic propagator is negative, given that $\xi_{\mathbf{k}} \approx \xi_{\mathbf{k}'}$, we have an effective attractive interaction between the electrons mediated by the nanopuddles. Remarkably, this interaction leads to the formation of finite center-of-mass momentum Cooper pairs represented by \mathbf{p} and \mathbf{p}' . Therefore, from the perspective of inhomogeneously distributed puddles bringing disorder to an otherwise clean medium, a bound state between two electrons can be formed with a finite center-of-mass momentum that is associated with the strenght of the interaction between the electrons forming the pair and the agglomeration of interstitial dopant oxygens in one nanopuddle.

It is important to notice that the states arising from the effective Hamiltonian in Eq. (2) are different from other proposed pair states with finite CM momentum, as for example the Fulde-Ferrell-Larkin-Ovchinnikov (FFLO) state, where finite center-of-mass momentum Cooper pairs can be stabilized under a finite magnetic field via the Zeeman coupling [46, 47], and the recently proposed current driven FFLO state [48]. Moreover, it has been shown that, even without the presence of a magnetic field or other external potentials, a finite CM momentum Cooper pair can be stable in a superconducting ground state as pointed in Ref. [7], but the authors do not explore the effects that can give rise to this kind of state. Here we start from the fact that nanosized puddles are formed via doping and the responsible for the CM momentum of the pairs is disorder induced by the puddles in the system.

Eventhough we are not considering any specific form for the interaction potential $g(\mathbf{k} - \mathbf{k}')$, it is important to comment that the only requirement is that it must be a finite size potential in real space, which means that is not a point-like disorder center that is scattering the electrons in the interaction term of Eq. (1), rather is a region in space defined by the agglomeration of oxygen interstitials. In this case, we can point to potentials like the Woods-Saxon potential [49] that is

Bragg diffraction patterns

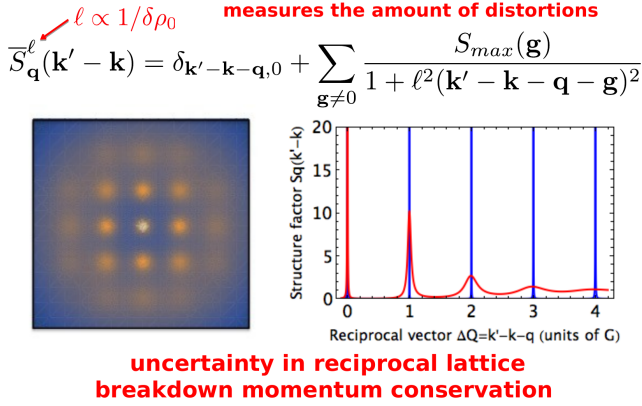


Figure 2. *Top*: Structure factor for disordered media from Hosemann’s paracrystalline theory [58], given by eq. (6) in the text. The pristine case corresponds to the $\ell \rightarrow \infty$ limit, where the structure factor is given by delta-peaks at reciprocal lattice vectors and momentum is conserved (here ℓ is a measure of disorder and for this reason should be inversely related to the residual resistivity shift due to structural disorder, $\ell \propto 1/\delta\rho_0$). *Bottom left*: – Bragg diffraction pattern for a structurally disordered medium, showing Bragg peaks at the central region and Bragg rings at the outer region; *Bottom right* – plot of the structure factor as a function of momentum transfer, $\Delta\mathbf{Q}$, showing well defined Bragg peaks, for small momentum transfer, at the reciprocal lattice vectors, \mathbf{G} , while the Bragg peaks become ever broader, at larger momentum transfer, eventually merging into rings.

used to describe the forces applied on protons and neutrons in the atomic nucleus or the Gogny-type interactions [50–52], which is another kind of nucleon-nucleon potential that has also found applications in astrophysics [53], as possible candidates to describe the electron-puddle interaction. However, a precise and detailed description of such potential would require more knowledge about the formation of the nanosized puddles and its effects on the crystal structure of the host material, which would affect the electronic degrees of freedom [54], but this is outside the scope of the present study.

III. STRUCTURAL DISORDER

Before we proceed to the characterization of the superconducting state that arises from the effective Hamiltonian derived in the last section, it is important to briefly discuss which kind of disorder is giving the Cooper pairs a finite CM momentum. In order to do that, we introduce concepts arising from the study of structural disorder, which is the kind of perturbation that the agglomeration of Oi causes in the crystalline structure of different cuprate systems, as for example by tilting the CuO_6 octahedra in $\text{La}_2\text{CuO}_{4+\delta}$ [55] and by altering the distance between the apical oxygen and the planar copper atom in $\text{Bi}_2\text{Sr}_2\text{CaCu}_2\text{O}_{8+\delta}$ [56].

Translational invariance is one of the most fundamental properties of pristine crystals. The concept of a Brillouin

zone, that repeats itself by translations of reciprocal lattice vectors, allows us to organize electrons in energy bands, $\epsilon_n(\mathbf{k})$, labeled by a band index, n , and function of a quasi-momentum (wave-vector) quantum number, \mathbf{k} , in terms of which periodic Bloch wave-functions, $u_{n,\mathbf{k}}(\mathbf{r})$, are defined. A perfect crystal is characterized by very intense and sharp peaks in the Fraunhofer diffraction pattern of Bragg scattering experiments. The existence of such sharp peaks follows directly from Heisenberg’s uncertainty principle and their location is determined by the crystalline-lattice structure factor. Simply put, an extended Bloch wave with well defined momentum state, \mathbf{k} , that interacts with ions located at arbitrary positions, \mathbf{r}_i , of the crystal (infinite uncertainty $\Delta\mathbf{r} \rightarrow \infty$), scatters into another extended Bloch wave with momentum state, \mathbf{k}' , with zero uncertainty, $\Delta\mathbf{k} \rightarrow 0$. The entire process carries a phase

$$\phi(\mathbf{k}' - \mathbf{k}) = \frac{1}{\sqrt{N}} \sum_{\mathbf{r}_i} f_{\mathbf{r}_i} e^{i(\mathbf{k}' - \mathbf{k}) \cdot \mathbf{r}_i}, \quad (3)$$

where N is the number of lattice sites in the crystal and $f_{\mathbf{r}_i}$ is an atomic form factor that gives the probability that an atom is located at a certain crystallographic position. The scattered intensity is proportional to $|\phi(\mathbf{k}' - \mathbf{k})|^2$ and is thus determined by the lattice structure factor,

$$S(\mathbf{k}' - \mathbf{k}) = \frac{1}{N} \sum_{\mathbf{r}_i, \mathbf{r}_j} f_{\mathbf{r}_i} f_{\mathbf{r}_j} e^{i(\mathbf{k}' - \mathbf{k}) \cdot (\mathbf{r}_i - \mathbf{r}_j)}. \quad (4)$$

For a pristine crystal all atoms are at their ideal locations, $f_{\mathbf{r}_i} = f_{\mathbf{r}_j} = 1$ and thus $S(\mathbf{k}' - \mathbf{k}) = \sum_{\mathbf{g}} \delta_{\mathbf{k}' - \mathbf{k}, \mathbf{g}}$, where \mathbf{g} is a reciprocal lattice vector. The Fraunhofer diffraction pattern in this case thus corresponds to δ -like peaks as shown in Fig. 2 and the kinematic constraint of quasi-momentum conservation,

$$\mathbf{k}' = \mathbf{k} + \mathbf{g}, \quad (5)$$

forms the basis for Bloch’s theorem. In the opposite limit of a random atom gas, however, an extended Bloch wave with well defined momentum state, \mathbf{k} , that interacts with ions located at a particular, well defined position, \mathbf{r}_i , of the crystal (zero uncertainty $\Delta\mathbf{r} \rightarrow 0$), scatters into another extended Bloch wave with momentum state, \mathbf{k}' , with infinite uncertainty, $\Delta\mathbf{k} \rightarrow \infty$. In this case, $f_{\mathbf{r}_i} f_{\mathbf{r}_j} = \delta_{\mathbf{r}_i, \mathbf{r}_j}$, and $S(\mathbf{q}) = 1$. There are no kinematic constraints whatsoever relating \mathbf{k} and \mathbf{k}' to \mathbf{g} and the Fraunhofer diffraction pattern in this case corresponds to an isotropic disc of even intensity, as shown in Fig. 2.

Interpolating between the pristine and random limits described above by increasing disorder is pivotal to the description of inherently inhomogeneous systems, such as the one of random oxygen puddles described in the present work. If disorder is of the first type, namely weak disorder, all atoms deviate only slightly from their ideal positions in the crystal, independently of the deviations of their neighbors [57]. This is the case of pointlike defects, thermal vibrations or micro-mechanical strains, and this kind of disorder preserves long range crystalline order. In this case the widths of the peaks in the Fraunhofer diffraction pattern are not affected,

and only their intensity is slightly reduced since for uncorrelated Gaussian disorder, $\bar{f}_{\mathbf{r}_i} \bar{f}_{\mathbf{r}_j} = D^2 < 1$, where D^2 is the Debye-Waller factor. The structure factor is given by $\bar{S}(\mathbf{k}' - \mathbf{k}) = D^2 \sum_{\mathbf{g}} \delta_{\mathbf{k}' - \mathbf{k}, \mathbf{g}}$. If disorder of the second type, namely strong disorder, however, the atoms deviate significantly from their ideal positions in the crystal, and deviations amongst neighboring atoms are correlated. This is the case of extended defects, amorphous regions, molten materials, etc, and this type of disorder causes the loss of long range crystalline order. In these paracrystalline structures, not only the intensity of the diffraction peaks will decrease but, most importantly, their widths will suffer from a nonlinear increase of their integral breadth, δg , for successive orders of Bragg reflections. The complete paracrystalline theory was proposed by Hosemann [58]. Hosemann included fluctuations of variance σ that introduce correlations between pairs of atoms, $\langle f_{\mathbf{r}_i} f_{\mathbf{r}_j} \rangle$, that decrease with separation ultimately causing the peaks in the structure factor of the material to broaden the larger the reciprocal lattice. The result is a structure factor composed by a sum of Lorentzians [59]

$$\bar{S}_{\mathbf{q}}(\mathbf{k}' - \mathbf{k}) = \sum_{\mathbf{g}} \frac{S_{max}(\mathbf{g})}{1 + \ell_{hkl}^2 (\mathbf{q} - \mathbf{k}' + \mathbf{k} - \mathbf{g})^2}, \quad (6)$$

of amplitudes $S_{max}(\mathbf{g}) = 4/\sigma^2 \mathbf{g}^2$ and breadths for Bragg reflections, $|\delta \mathbf{g}| \equiv 1/\ell_{hkl} = \sigma^2 \pi^2 (h^2 + k^2 + l^2)/a_0$, given in terms of the original lattice parameter a_0 and the momentum transfer, \mathbf{q} . Hosemann's paracrystalline theory allows us then to interpolate continuously between pristine and random cases through the fluctuation parameter σ :

- for $\sigma \rightarrow 0$ we have $\ell_{hkl} \rightarrow \infty, \forall h, k, l$ and we obtain $\bar{S}_{\mathbf{q}}(\mathbf{k}' - \mathbf{k}) = \sum_{\mathbf{g}} \delta_{\mathbf{q}, \mathbf{k}' - \mathbf{k} + \mathbf{g}}$, enforcing the kinematic constraint of momentum conservation, $\mathbf{q} = \mathbf{k}' - \mathbf{k} + \mathbf{g}$, typical of pristine crystals [59];
- for $\sigma \rightarrow \infty$ we have $\ell_{hkl} \rightarrow 0, \forall h, k, l$ and we end up with $\bar{S}_{\mathbf{q}}(\mathbf{k}' - \mathbf{k}) = S_{max}(\mathbf{0}) \rightarrow 1$, isotropic, for arbitrary $\mathbf{q}, \mathbf{k}, \mathbf{k}'$ and determined solely by the $\mathbf{g} = \mathbf{0}$ contribution, typical of infinite, aperiodic systems [59];
- for $0 \leq \sigma \leq \infty$ we have $\infty \geq \ell_{hkl} \geq 0$ and the structure factor, $\bar{S}_{\mathbf{q}}(\mathbf{k}' - \mathbf{k})$, will be composed by sharp Bragg peaks at small \mathbf{g} (large ℓ_{hkl}) and isotropic discs for larger \mathbf{g} (small ℓ_{hkl}), as shown in Fig. 2, relaxing the kinematic constraint of momentum conservation, $\mathbf{q} \neq \mathbf{k}' - \mathbf{k} + \mathbf{g}$, typical of a paracrystal, liquids, strongly disordered or amorphous systems [59].

IV. DISORDER AND GAP FLUCTUATIONS

We now address how the superconducting state of the effective interaction derived in Sec. II is affected by the structural disorder effects introduced in the previous section. We start from the effective Hamiltonian in Eq. (2) and, within a mean-field decoupling of the quartic term, write the equation for the superconducting gap as

$$\Delta_{\mathbf{k}} = - \sum_{\mathbf{k}', \mathbf{p}'} V_{\mathbf{k}, \mathbf{k}'} f_{\mathbf{0}, \mathbf{p}'} \langle c_{\mathbf{p}' - \mathbf{k}' \downarrow} c_{\mathbf{k}' \uparrow} \rangle, \quad (7)$$

where we set $\mathbf{p} = \mathbf{0}$, since we want to describe amplitude fluctuations for the superconducting gap in the Cooper channel. For the superconducting state formed by singlet pairs with finite CM momentum, the system can be represented by the spin-independent imaginary time Green's function $\mathcal{G}(\mathbf{k}, \mathbf{k}', \tau) = - \langle T_{\tau} c_{\mathbf{k}, \sigma}(\tau) c_{\mathbf{k}', \sigma}^{\dagger}(0) \rangle$ and the anomalous pair propagators $\mathcal{F}(\mathbf{k}, \mathbf{k}', \tau) = \langle T_{\tau} c_{\mathbf{k}, \sigma}(\tau) c_{\mathbf{k}' \sigma'}(0) \rangle$ and $\mathcal{F}^*(\mathbf{k}, \mathbf{k}', \tau) = \langle T_{\tau} c_{\mathbf{k}, \sigma}^{\dagger}(\tau) c_{\mathbf{k}' \sigma'}^{\dagger}(0) \rangle$ for $\sigma \neq \sigma'$. Within Nambu's formalism, we can write the decoupled effective Hamiltonian from Eq. (2) and the electronic components from H_{el} in matrix form and derive in first order perturbation theory the electronic Green's function for an inhomogeneous system with disorder as

$$\begin{aligned} \mathbf{G}(\mathbf{k}, \mathbf{k}', i\omega_n) &= \mathbf{G}_0(\mathbf{k}, \mathbf{k}', i\omega_n) \\ &+ \sum_{\mathbf{p}, \mathbf{p}'} \mathbf{G}_0(\mathbf{k}, \mathbf{p}, i\omega_n) \mathcal{T}_{\mathbf{p}, \mathbf{p}'} \sigma_3 \mathbf{G}(\mathbf{p}', \mathbf{k}', i\omega_n), \end{aligned}$$

where $\mathbf{G}_0(\mathbf{k}, \mathbf{k}', i\omega_n)$ is the matrix form of the translationally invariant electronic Green's function in frequency space, $i\omega_n$ are the fermionic Matsubara frequencies and σ_3 is a Pauli matrix. The diagonal elements of this matrix are defined by the bare Green's function in the superconducting state, $\mathcal{G}_0(\mathbf{k}, i\omega_n)$, and its off-diagonal terms are represented by the anomalous propagators $\mathcal{F}_0(\mathbf{k}, i\omega_n)$ which are written as

$$\begin{aligned} \mathcal{G}_0(\mathbf{k}, i\omega_n) &= \frac{-(i\omega_n + \xi_{\mathbf{k}})}{\omega_n^2 + \xi_{\mathbf{k}}^2 + |\Delta_{\mathbf{k}}|^2}, \\ \mathcal{F}_0(\mathbf{k}, i\omega_n) &= \frac{\Delta_{\mathbf{k}}}{\omega_n^2 + \xi_{\mathbf{k}}^2 + |\Delta_{\mathbf{k}}|^2}. \end{aligned}$$

In order to proceed, we shall take a couple of approximations: first we consider the case of overdoped cuprates, which puts the system in a high concentration of disorder, thus $\mathcal{T}_{\mathbf{p}, \mathbf{p}'} = \mathcal{T} f(\mathbf{p}, \mathbf{p}')$, where disorder influences the momentum transfer controlled by the phase factor $f(\mathbf{p}, \mathbf{p}')$ with strenght \mathcal{T} . Second we assume that for a translationally invariant system the normal and anomalous Green's functions can be rewritten as $\mathcal{G}_0(\mathbf{k}, \mathbf{k}', i\omega_n) = \mathcal{G}_0(\mathbf{k}, i\omega_n) \delta_{\mathbf{k}, \mathbf{k}'}$ and $\mathcal{F}_0(\mathbf{k}, \mathbf{k}', i\omega_n) = \mathcal{F}_0(\mathbf{k}, i\omega_n) \delta_{-\mathbf{k}, \mathbf{k}'}$. Following these couple of approximations, the first order perturbation theory expansion of the interacting Green's function is simplified

$$\begin{aligned} \mathbf{G}(\mathbf{k}, \mathbf{k}', i\omega_n) &= \mathbf{G}_0(\mathbf{k}, i\omega_n) \delta_{\mathbf{k}, \mathbf{k}'} \\ &+ \mathcal{T} f_{\mathbf{k}, \mathbf{k}'} \mathbf{G}_0(\mathbf{k}, i\omega_n) \sigma_3 \mathbf{G}_0(\mathbf{k}', i\omega_n). \end{aligned} \quad (8)$$

From the gap equation in Eq. (7) and from the definition of the anomalous propagator, we write

$$\begin{aligned}\Delta_{\mathbf{k}} &= - \sum_{\mathbf{k}', \mathbf{p}'} V_{\mathbf{k}, \mathbf{k}'} f_{0, \mathbf{p}'} \langle c_{\mathbf{p}' - \mathbf{k}' \downarrow} c_{\mathbf{k}' \uparrow} \rangle \\ &= - \sum_{\mathbf{k}', \mathbf{p}'} V_{\mathbf{k}, \mathbf{k}'} f_{0, \mathbf{p}'} \left[\frac{1}{\beta} \sum_{\omega_n} \mathcal{F}(\mathbf{p}' - \mathbf{k}', \mathbf{k}', i\omega_n) \right],\end{aligned}\quad (9)$$

with $\beta = 1/T$ being the inverse temperature (in units of $k_B = 1$). By using the matrix form in Eq. (8), we get the form of the interacting anomalous propagator, where it is worth noting that the normal and anomalous propagators mix in the impurity scattering. Despite the anomalous Green's function being invariant for time reversal, the normal one is not, and since disorder produces the transformation $\mathcal{F}_0(\mathbf{k}, i\omega_n) \leftrightarrow \mathcal{G}_0(\mathbf{k}, i\omega_n)$ we clearly see this is a mechanism that breaks time reversal invariance. As a consequence, this mechanism breaks the Cooper pair that leaks into the normal metal surrounding the puddles.

In order to understand the effects of disorder and finite CM momentum in the gap equation, we substitute the form of the anomalous propagator given by the matrix in Eq. (8) inside Eq. (9) to write the gap equation as $\Delta_{\mathbf{k}} = \Delta_{\mathbf{k}}^{\text{BCS}} + \delta\Delta_{\mathbf{k}}$, where

$$\Delta_{\mathbf{k}}^{\text{BCS}} = - \sum_{\mathbf{k}'} \frac{V_{\mathbf{k}, \mathbf{k}'} \Delta_{\mathbf{k}'}}{2E_{\mathbf{k}'}} \tanh\left(\frac{\beta E_{\mathbf{k}'}}{2}\right), \quad (10)$$

is the BCS limit for the gap equation, arising from the first term in Eq. (8), with the bare anomalous propagators and $E_{\mathbf{k}} = \sqrt{\xi_{\mathbf{k}}^2 + \Delta_{\mathbf{k}}^2}$. Then

$$\delta\Delta_{\mathbf{k}} = \mathcal{T} \sum_{\mathbf{k}', \mathbf{p}'} V_{\mathbf{k}, \mathbf{k}'} f_{0, \mathbf{p}'} f_{\mathbf{p}', 0} \frac{1}{\beta} \sum_{\omega_n} \{\mathcal{F}_0 \mathcal{G}_0 + \mathcal{G}_0 \mathcal{F}_0\} \quad (11)$$

is the correction to the superconductor gap due to effects of disorder in the system. The factor $[f_{0, \mathbf{p}'} f_{\mathbf{p}', 0}]$ can be treated within a mean over disorder in order to calculate the interference factor as $[f_{0, \mathbf{p}'} f_{\mathbf{p}', 0}] = |f_{0, \mathbf{p}'}|^2 \rightarrow S(\mathbf{p}')$, where $S(0, \mathbf{p}')$ is the static structure factor. Thus, the correction to the gap equation can be written in terms of the structure factor and we see that fluctuations associated with small CM momentum $\mathbf{p}' \rightarrow 0$ are absent, since the structure factor $S(\mathbf{p}') \rightarrow 0$ and the gap equation is dominated by the BCS contribution. On the other hand, fluctuations associated with a finite center-of-mass momentum dominate over the BCS contribution when $\mathbf{p}' \gg 0$ and $S(\mathbf{p}') \rightarrow 1$. In a general manner, the structure factor can be written as a sum of Lorentzians with peaks in wave vectors of the reciprocal lattice, as discussed in Sec. III and shown in Fig. 2.

Finally, we proceed by taking the Matsubara summations over the set of mixed Green's functions as in Eq. (11) to arrive at the correction in terms of the disorder strength \mathcal{T} and the finite CM momentum of the Cooper pairs \mathbf{p}' as

$$\begin{aligned}\delta\Delta_{\mathbf{k}} &= \mathcal{T} \sum_{\mathbf{k}', \mathbf{p}'} V_{\mathbf{k}, \mathbf{k}'} S(\mathbf{p}') \frac{1}{2} \left[\frac{\Delta_{\mathbf{k}', \mathbf{p}'}}{E_{\mathbf{k}' - \mathbf{p}'}} \frac{\xi_{\mathbf{k}'}}{E_{\mathbf{k}'}} + \frac{\Delta_{\mathbf{k}'}}{E_{\mathbf{k}'}} \frac{\xi_{\mathbf{k}' - \mathbf{p}'}}{E_{\mathbf{k}' - \mathbf{p}'}} \right] \\ &\times \left\{ \frac{E_{\mathbf{k}' - \mathbf{p}'} \tanh\left(\frac{\beta E_{\mathbf{k}'}}{2}\right) - E_{\mathbf{k}'} \tanh\left(\frac{\beta E_{\mathbf{k}' - \mathbf{p}'}}{2}\right)}{E_{\mathbf{k}' - \mathbf{p}'}^2 - E_{\mathbf{k}'}^2} \right\}.\end{aligned}\quad (12)$$

It is important to notice the dependence of the correction on the structure factor $S(\mathbf{p}')$ controlling momentum transfer. In the limit of small amount of disorder, the so called first-type disorder [57], as discussed in Sec. III, pointlike defects does not affect the BCS gap, in accordance with Anderson's Theorem, as we shall see in the next section. On the other hand, in the limit of high concentration of puddles, the system is in the limit of second-type disorder, associated with strain-induced lattice deformations, and both the amplitude of the superconducting gap and the critical temperature are affected.

In order to proceed to the numerical analysis, we perform an approximation for the structure factor based on the limits of disorder discussed above. For the first-type disorder, we choose $S(\mathbf{p}') = \delta_{0, \mathbf{p}'}$, since no momentum transfer will be associated with pairs with finite CM momentum in the dilute limit. On the other hand, for the second-type disorder, we write $S(\mathbf{p}') = 1$, assuming a system with high concentration of puddles. These two limits for the disorder of the 1st and 2nd types can be understood as a *hard cutoff* for the CM momentum distribution within the structure factor and are made to simplify Eq. (12) to the following numerical analysis.

V. NUMERICAL ANALYSIS

In order to fully understand the effects of disorder and CM momentum of the Cooper pairs in the superconducting gap amplitude we perform a numerical integration of Eq. (12). We use the decomposition $V_{\mathbf{k}, \mathbf{k}'} = -V_0 \eta(\mathbf{k}) \eta(\mathbf{k}')$ and $\Delta_{\mathbf{k}} = \Delta_0 \eta(\mathbf{k})$, where $\eta(\mathbf{k}) = \cos k_x - \cos k_y$ is a d -wave form factor, which gives the amplitude fluctuations of the order parameter with the same symmetry. When stated for comparison, we shall also use $V_{\mathbf{k}, \mathbf{k}'} = -V_0$ and $\Delta_{\mathbf{k}} = \Delta_0$ when considering a s -wave symmetry for the interaction and the gap. For the calculations in the square lattice, we consider a two-dimensional electronic dispersion with nearest- and next-nearest-neighbor hopping elements (t, t') as

$$\epsilon_{\mathbf{k}} = -2t(\cos k_x + \cos k_y) + 4t' \cos k_x \cos k_y - \mu, \quad (13)$$

where μ is the chemical potential that controls the electronic density. This type of electronic dispersion is general for 2D transport in strongly correlated systems and is suitable for the description of the conduction band associated with the CuO_2 planes of high- T_c cuprates.

In the following calculations, all parameters are defined in units of $4t$ and we set $\mu/4t = -0.45$, away from the half-filled case $\mu/4t = 0.0$ (see Fig. 3), since the mean-field theory

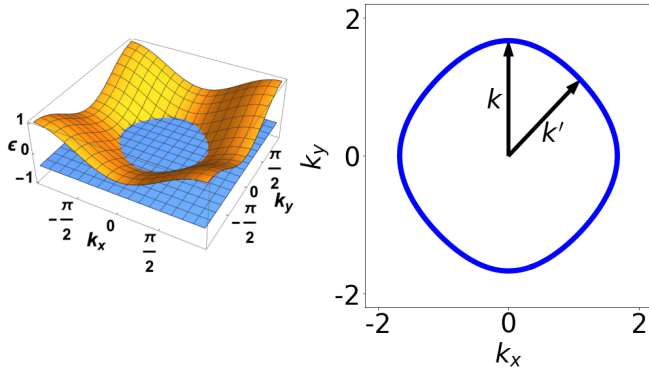


Figure 3. Fermi surface structure used in calculations. *Left*: The 3D plot of Eq. (13) in the first Brillouin zone in yellow and the chemical potential cut defining the Fermi level in blue. *Right*: The Fermi level defined by the cut at $\mu/4t = -0.45$. The vectors \mathbf{k} , fixed in the direction $(0, \pi)$, and \mathbf{k}' , varying across the Fermi surface, are also shown.

yields incorrect results for a two-dimensional lattice near half-filling [60] and we avoid particle-hole symmetry [61]. For this reason, we can take $t' = 0$. We also set $V_0/4t = 1.0$, in the limit where the mean-field theory is still valid. For the summations over \mathbf{p}' , we define $\mathbf{p}' = \mathbf{k} - \mathbf{k}'$, where \mathbf{k}, \mathbf{k}' are the momenta of the two paired electrons, which we set $|\mathbf{k}| = |\mathbf{k}'| = k_F$ as two momenta in the Fermi surface. The CM momenta are then defined by fixing \mathbf{k} in the direction of the point $(0, \pi)$ and by varying \mathbf{k}' across the Fermi surface, as shown in Fig. 3.

We start by analyzing the zero temperature limit $T = 0$ of Eq. (12), where the hyperbolic tangents can be simplified. In Fig. 4 we show how the gap amplitude Δ_0 is affected by disorder \mathcal{T} in the limit of disorder of the 1st type, $S(\mathbf{p}') = \delta_{0,\mathbf{p}'}$, or weak concentration of puddles, and strong concentration, $S(\mathbf{p}') = 1$, in the limit of disorder of the 2nd kind. The gap amplitude is insensitive to disorder in the dilute limit for s -wave pairing, thus $\Delta_0 = \Delta_0^{\text{BCS}}$ and the BCS limit is recovered, in accordance with Anderson's theorem. However, in the opposite limit, the disorder strongly affects the amplitude of the gap for d -wave pairing, introducing fluctuations and decreasing its absolute value in about 50% in the strong disorder limit, when compared to the clean case.

It is worth noting that the reduction is not linear as the strength of disorder approaches the values of the fixed pairing potential, $\mathcal{T} \rightarrow V_0$, where the perturbation theory still holds. This can be traced back to the fact that the gap equation is a self-consistent equation for the absolute value of Δ_0 , even after the approximations considered. Thus we see that even in the zero temperature limit, disorder tends to destroy superconductivity in a system with high concentration of oxygen interstitials, as in the overdoped cuprates.

We also investigate the effects of specific finite CM momentum on the amplitude of the gap when $T = 0$. We choose a set of momenta $\{\mathbf{p}\}$ and substitute in Eq. (12) the corresponding structure factor, namely $S(\mathbf{p}_s) = \delta_{\mathbf{p}',\mathbf{p}_s}$, where \mathbf{p}_s are the momenta in the set. All \mathbf{p}_s are multiples of \mathbf{k}_F of each direction considered, namely $(0, \pi)$ and (π, π) . In Fig. 5 we display the

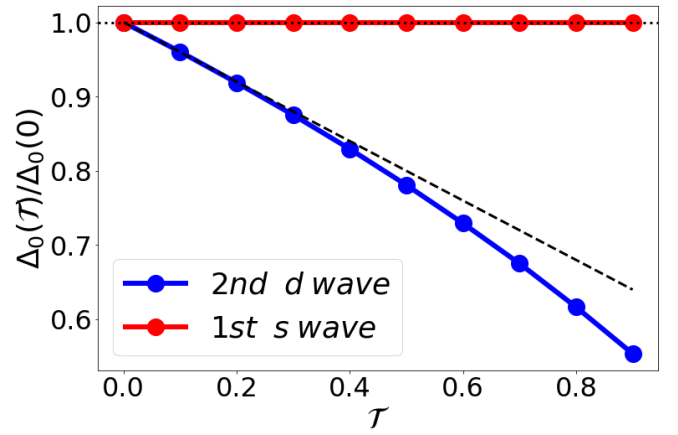


Figure 4. $T = 0$ limit for the amplitude fluctuations of the superconducting gap as a function of disorder strength compared to the clean system. Dilute limit (red), for disorder of the 1st kind and s -wave symmetry, and high concentration of puddles for disorder of the 2nd kind and d -wave symmetry (blue). The black dashed line is a guide to the eye. Gap values are given in terms of Δ_0 in the absence of disorder $\mathcal{T} = 0$.

evolution of the amplitude of the superconducting order parameter Δ_0 as a function of the CM momentum of the Cooper pairs \mathbf{p} , for fixed disorder strength $\mathcal{T} = 0.1$. The superconducting order parameter is modulated, with period determined by the distance between adjacent Fermi surfaces in each direction, being $3.75|\mathbf{k}_F|$ for $(0, \pi)$ and $5.75|\mathbf{k}_F|$ for (π, π) . Remarkably, this is in direct contact with the diffraction pattern displayed in Fig. 2. However, since we are considering a hard cutoff for the structure factor in terms of delta functions, the amplitude of the gap modulation is not altered by the distance from the origin. We expect that by including a more realistic model for the structure factor, the amplitudes of the modulations will decay with \mathbf{p} , with its effect stronger in the (π, π) direction, since larger reciprocal lattice vectors \mathbf{G} imply a broader structure factor, thus diminishing the amplitude of the superconducting gap. Altogether, the interplay between disorder and finite center-of-mass momentum Cooper pairs is able to strongly affect the superconducting order parameter.

Now we turn to the finite temperature case $T \neq 0$ for the d -wave symmetric order parameter to understand how disorder and CM momenta for the Cooper pairs affects the critical temperature T_c . In Fig. 6 we show the evolution of the superconducting gap with temperature, for different values of the disorder strength \mathcal{T} . It is clear that with increasing disorder, not only $\Delta_0(0)$ decreases, as pointed in the zero temperature limit, but we also evidence a decrease in the critical temperature T_c , defined as the value of temperature that $\Delta_0(T, \mathcal{T}) \rightarrow 0$, with disorder, as shown in the inset. This means that pair breaking is induced by the scattering of the finite CM momentum Cooper pairs with the nanosized oxygen puddles of the system and by increasing disorder, T_c is significantly reduced.

This pair breaking effect is due to the fact that the phase space required to pair formation is reduced when \mathbf{p} increases in absolute value. In the small scattering momentum transfer

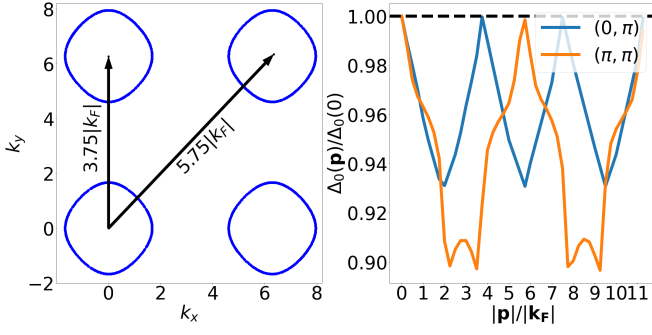


Figure 5. *Left*: Extended Brillouin zones in the upper positive part of momentum space. The arrows indicate the distance between the centers of each Fermi surface in terms of the Fermi vector $|k_F|$ of each direction considered. *Right*: The amplitude of the superconducting order parameter as a function of different CM momentum vectors $|\mathbf{p}|$, in the directions $(0, \pi)$ and (π, π) . $\Delta_0(\mathbf{p})$ is given in units of the gap at $\mathbf{p} = 0$.

sector, $\mathbf{p} < |\mathbf{k}_F|$, the gap is almost unaffected by the presence of disorder when compared to the value when $\mathbf{p} = 0$, since the shape of the Fermi surface intersection of the two paired electrons suffers little change. However, when \mathbf{p} approaches the maximum absolute value of $2|\mathbf{k}_F|$ within the first Brillouin zone, the phase space for pair formation is greatly reduced and disorder induces pair breaking, captured by the reduction of the superconducting order parameter. The modulation occurs for $\mathbf{p} > 2|\mathbf{k}_F|$, since electrons from different Brillouin zones participate in the scattering and pairing process. Therefore, these results point to the combined effect of finite center-of-mass momentum pairs being scattered by structural disorder induced by the network of oxygen puddles as a mechanism for the reduction of the superconducting gap and the critical temperature in the overdoped regime.

VI. CONCLUSION AND DISCUSSION

In this work we presented an extension of the proposed model for the formation of networks of puddles and its effects on the superconductivity in oxygen-doped cuprates [38]. We show that the presence of puddles, in the overdoped side of the phase diagram, introduces strong disorder in the system that induces the formation of finite center-of-mass momentum Cooper pairs. We derive an analytical expression for the amplitude fluctuations in the superconducting gap induced by the puddles, within a mean-field BCS-like approach, in terms of the disorder strength \mathcal{T} and the finite CM momenta \mathbf{p} . We numerically solve this expression to show that even in the zero temperature limit the gap is strongly affected by disorder-induced CM Cooper pairs. In the limit of strong disorder, the gap tends to close and, in the finite temperature case, T_c tracks the reduction of the superconducting gap, also being strongly affected by disorder. It is important to emphasize that we do not account the effect of longer-range Coulomb repulsion, restricting the application of our results to screened systems [68].

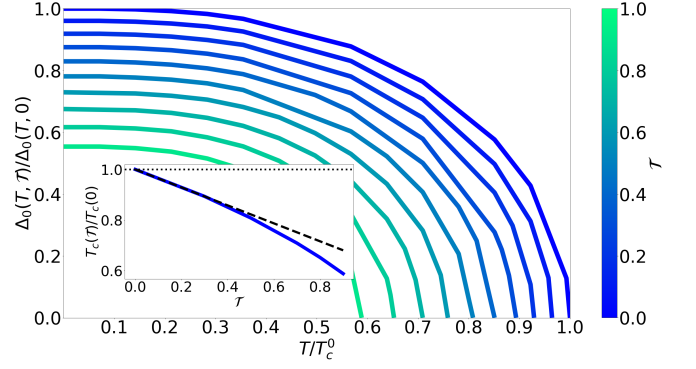


Figure 6. Temperature dependence of the superconducting order parameter for different values of disorder strength (colored bar). Gap values are given in terms of the clean case $\mathcal{T} = 0$ and temperature in terms of T_c^0 also of the clean case. *Inset*: The critical temperature dependence normalized to the clean value as a function of disorder strength. The black dashed line is a guide to the eye.

The experimental observations of structural scale invariance of dopants detected by scanning micro-x-ray diffraction [36], the promotion of critical temperature [37], the agglomeration of interstitial oxygens in regions of strong local strain in the crystal structure of cuprate superconductors [42, 43] and the proposed theoretical reports regarding the presence of networks of nanoscale superconducting islands in high-temperature superconductors [62–65] are in close connection with the results reported here. Eventhough we are showing that the superconducting state is depleted in the presence of strong disorder in the overdoped regime, it is clear from the above mentioned surveys that the importance of these networks and its interplay with electronic degrees of freedom pass across the whole phase diagram of hole-doped cuprates.

In Ref. [38], the present authors show how the complex networks formed by the oxygen puddles can transionate to a synchronized phase, controlled by the superfluid density, in a way that the concentration of dopant atoms controls the emergence of local superconductivity in the underdoped regime and how the systems evolves to a bulk superconductor as the concentration of dopants, thus puddles, increases as the systems approaches the optimally doped regime. It is important to emphasize that within this framework, the state studied in this work is described by the bulk superconductor state in the synchronized phase of the network formed by the oxygen puddles (see Fig. 1), in the sense that we require the network of puddles to be fully synchronized in order to the band of electrons to interact with the global mode of vibration of the synchronized network. Our approach is based on a mean-field approximation for the complex network, therefore we point to the importance of describing different topologies for the organization of the puddles and how this can affect not only the transition to the superconducting state [66], but also its possible interplay with the superconducting fluctuations of pre-formed Cooper pairs observed in the pseudogap phase above T_c [67], in terms of local superconductivity.

Appendix A: Unitary transformation

In this Appendix section, we show the derivation of the effective Hamiltonian containing the pairing interaction between two electrons forming a Cooper pair with finite center-of-mass momentum. The starting point is the full Hamiltonian written in momentum space $H = H_{el} + H_p + H_{el-p}$, which is the summation over the contributions of the electrons, puddles and electron-puddle interaction, respectively. Introducing an unitary transformation of the form $H' = e^{-S} H e^S$, where S is the transformation matrix introduced in Sec. II, we can expand the exponentials up to second order in powers of S to write the transformed Hamiltonian as

$$H' = H + [H, S] + \frac{1}{2} [[H, S], S], \quad (A1)$$

and by treating H_{el-p} as a perturbation, we can divide the full Hamiltonian as $H = H_0 + H_{el-p}$, where H_0 contains the kinetic terms of electrons and puddles, to write

$$H' = H_0 + H_{el-p} + [H_0, S] + [H_{el-p}, S] + \frac{1}{2} [[H_0, S], S].$$

Since the goal is to eliminate the interaction, the defining equation for the transformation matrix comes from the elimination of the first-order term $[H_0, S] + H_{el-p} = 0$, from which we can extract the factors x and y for S . In this way, the transformed Hamiltonian can be written in terms of an effective interaction that comes from recombining the terms in the commutators

$$H' = H_0 + \frac{1}{2} [H_{el-p}, S], \quad (A2)$$

thus the problem is reduced to an effective system described by $H = H_0 + H_{eff}$, where $H_{eff} = \frac{1}{2} [H_{el-p}, S]$. By performing the calculation over the commutator $[H_0, S]$, the choice of x and y that eliminate the first-order term is given by

$$x_{\mathbf{k}, \mathbf{k}', \mathbf{q}} = \frac{1}{\xi_{\mathbf{k}'} - \xi_{\mathbf{k}} - \omega_{\mathbf{q}}},$$

$$y_{\mathbf{k}, \mathbf{k}', \mathbf{q}} = \frac{1}{\xi_{\mathbf{k}'} - \xi_{\mathbf{k}} + \omega_{\mathbf{q}}},$$

and the transformation matrix S is fully defined. Then we proceed to the calculation of the effective Hamiltonian that comes from the commutator of the now defined matrix S and the electron-puddle interaction, which gives a combination of $M(\mathbf{q}, \mathbf{Q})M(-\mathbf{q}, \mathbf{Q}')$, where $\mathbf{Q} = \mathbf{k} - \mathbf{k}'$ and $\mathbf{Q}' = \mathbf{k}'' - \mathbf{k}'''$ are two auxiliar variables that accomodate the variety of indices arising from the commutator. Recalling the definition of the factor M given in the main text, we see that

$$M(\mathbf{q}, \mathbf{Q})M(-\mathbf{q}, \mathbf{Q}') = \sum_{\mathbf{R}, \mathbf{R}'} g(\mathbf{Q})g(\mathbf{Q}') \times e^{i(\mathbf{R}-\mathbf{R}') \cdot \mathbf{q}} e^{-i(\mathbf{Q} \cdot \mathbf{R} + \mathbf{Q}' \cdot \mathbf{R}')},$$

which can be simplified by taking $\mathbf{R} = \mathbf{R}'$ since each \mathbf{R} describes the position of a nanosized puddle and we are assuming the dilute limit of oxygen puddles, as discussed in the main text, in accordance with STEM and STM measurements [42, 43]. In this way, the effective Hamiltonian is written as

$$H_{eff} = \sum_{\mathbf{k}', \mathbf{k}''', \mathbf{q}, \mathbf{Q}, \mathbf{Q}'} V(\mathbf{q}, \mathbf{Q}, \mathbf{Q}') M(\mathbf{q}, \mathbf{Q}) M(-\mathbf{q}, \mathbf{Q}') \times c_{\mathbf{k}'''+\mathbf{Q}}^\dagger c_{\mathbf{k}'+\mathbf{Q}}^\dagger c_{\mathbf{k}'} c_{\mathbf{k}'''}, \quad (A3)$$

with $V(\mathbf{q}, \mathbf{Q}, \mathbf{Q}') = \omega_{\mathbf{q}} / [(\xi_{\mathbf{k}'''} - \xi_{\mathbf{k}'''+\mathbf{Q}'} - \omega_{\mathbf{q}})^2 - \omega_{\mathbf{q}}^2]$. Proceeding with the calculation, we note that within BCS theory, the effective Hamiltonian describes the interaction between electrons with opposite momenta $\mathbf{k}' = -\mathbf{k}'''$, with zero CM momentum. However, in our case, the auxiliar variables \mathbf{Q} and \mathbf{Q}' introduces a momentum transfer connected with a finite CM momentum for the pairs, for each fermionic operator in the effective Hamiltonian that comes from the commutator $[H_{el-p}, S]$. In this sense, we perform a change of variables introducing the finite CM momentum $\mathbf{k}' + \mathbf{k}''' = \mathbf{p}$, in a way that we can eliminate the dependence on the auxiliar variables. The new variables introduced are written as $\mathbf{k} = \mathbf{k}''' + \mathbf{Q}'$ and $-\mathbf{k} + \mathbf{p}' = \mathbf{k}' + \mathbf{Q}$, where \mathbf{p} and \mathbf{p}' are the CM momenta of the Cooper pairs. In the limit where the interaction $g(\mathbf{k}, \mathbf{k}')$ is independent of the CM momenta, we can decouple the effective interaction and end up with the effective Hamiltonian

$$H_{eff} = \sum_{\mathbf{k}, \mathbf{k}'} \sum_{\mathbf{p}, \mathbf{p}'} V(\mathbf{k}, \mathbf{k}') f(\mathbf{p}, \mathbf{p}') c_{\mathbf{k}, \uparrow}^\dagger c_{\mathbf{p}-\mathbf{k}, \downarrow}^\dagger c_{\mathbf{p}'-\mathbf{k}', \downarrow} c_{\mathbf{k}', \uparrow},$$

with

$$V(\mathbf{k}, \mathbf{k}') = \frac{\omega_0}{(\xi_{\mathbf{k}'} - \xi_{\mathbf{k}})^2 - \omega_0^2} |g(\mathbf{k} - \mathbf{k}')|^2$$

$$f(\mathbf{p}, \mathbf{p}') = \sum_{\mathbf{R}} e^{-i(\mathbf{p}' - \mathbf{p}) \cdot \mathbf{R}}$$

where we assume $\omega_{\mathbf{q}} = \omega_0$, a dispersionless phonon mode for each puddle.

-
- [1] J. Bardeen, L. N. Cooper, and J. R. Schrieffer, Theory of Superconductivity. *Phys. Rev.* **108**, 1175 (1957)
- [2] D. F. Agterberg, J. S. Davis, S. D. Edkins, E. Fradkin, D. J. Van Harlingen, S. A. Kivelson, P. A. Lee, L. Radzihovsky, J. M. Tranquada, and Y. Wang, The Physics of Pair-Density Waves: Cuprate Superconductors and Beyond. *Annu. Rev. Condens. Matter Phys.* **11**, 231 (2020).
- [3] Y. Wang, D. F. Agterberg, and A. Chubukov, Coexistence of Charge-Density-Wave and Pair-Density-Wave Orders in Underdoped Cuprates. *Phys. Rev. Lett.* **114**, 197001 (2015).
- [4] D. Chakraborty, M. Grandadam, M. H. Hamidian, J. C. S. Davis, Y. Sidis, and C. P. epin, Fractionalized pair density wave in the pseudogap phase of cuprate superconductors. *Phys. Rev. B* **100**, 224511 (2019).
- [5] J. Wardh and M. Granath, Effective model for a supercurrent in a pair-density wave. *Phys. Rev. B* **96**, 224503 (2017).
- [6] P. Choubey, S. H. Joo, K. Fujita, Z. Du, S. D. Edkins, M. H. Hamidian, H. Eisaki, S. Uchida, A. P. Mackenzie, J. Lee, J. C. S. Davis, and P. J. Hirschfeld, Atomic-scale electronic structure of the cuprate pair density wave state coexisting with superconductivity. *Proc. Natl. Acad. Sci. USA* **117**, 14805 (2020).
- [7] Florian Loder, Arno P. Kampf, and Thilo Kopp, Superconducting state with a finite-momentum pairing mechanism in zero external magnetic field. *Phys. Rev. B* **81**, 020511(R) (2010)
- [8] M. H. Hamidian, S. D. Edkins, S. H. Joo, A. Kostin, H. Eisaki, S. Uchida, M. J. Lawler, E.-A. Kim, A. P. Mackenzie, K. Fujita, J. Lee, and J. C. S. Davis, Detection of a Cooper-pair density wave in $\text{Bi}_2\text{Sr}_2\text{CaCu}_2\text{O}_{8+x}$. *Nature* **532**, 343 (2016)
- [9] X. Liu, Y. X. Chong, R. Sharma, and J. C. S. Davis, Discovery of a Cooper-pair density wave state in a transition-metal dichalcogenide. *Science* **372**, 1447 (2021).
- [10] H. Chen *et al.* Roton pair density wave in a strong-coupling kagome superconductor. *Nature* **599**, 222 (2021).
- [11] Angela Q. Chen, Moon Jip Park, Stephen T. Gill, Yiran Xiao, Dalmau Reig-i-Plessis, Gregory J. MacDougall, Matthew J. Gilbert and Nadya Mason, Finite momentum Cooper pairing in three-dimensional topological insulator Josephson junctions. *Nature Communications* **9**, 3478 (2018)
- [12] S. D. Edkins, A. Kostin, K. Fujita, A. P. Mackenzie, H. Eisaki, S. Uchida, S. Sachdev, M. J. Lawler, E.-A. Kim, J. C. Seamus Davis, and M. H. Hamidian, Magnetic field-induced pair density wave state in the cuprate vortex halo. *Science* **364**, 976 (2019)
- [13] I. A. Semenikhin, Influence of disordering on the critical temperature of superconductors with a short coherence length. *Physics of the Solid State* **45**, 1622 (2003)
- [14] Debmalya Chakraborty and Annica M. Black-Schaffer, Interplay of finite-energy and finite-momentum superconducting pairing. *Phys. Rev. B* **106**, 024511 (2022)
- [15] J.-J. Wen *et al.* Observation of two types of charge-density-wave orders in superconducting $\text{La}_{2-x}\text{Sr}_x\text{CuO}_4$. *Nature Communications* **10**, 3269 (2019)
- [16] K. McElroy, H. Eisaki, S. Uchida, and S. C. Davis, Atomic-Scale Sources and Mechanism of Nanoscale Electronic Disorder in $\text{Bi}_2\text{Sr}_2\text{CaCu}_2\text{O}_{8+\delta}$. *Science* **309**, 1048 (2005).
- [17] Nicola Poccia, Matthieu Chorro, Alessandro Ricci, Wei Xu, Augusto Marcelli, Gaetano Campi, Antonio Bianconi, Percolative superconductivity in $\text{La}_2\text{CuO}_{4.06}$ by lattice granularity patterns with scanning micro x-ray absorption near edge structure. *Appl. Phys. Lett.* **104**, 221903 (2014)
- [18] Alessandro Ricci *et al.* Networks of superconducting nanopuddles in 1/8 doped $\text{YBa}_2\text{Cu}_3\text{O}_{6.5+y}$ controlled by thermal manipulation. *New J. Phys.* **16**, 053030 (2014)
- [19] E. W. Huang, D. J. Scalapino, T. A. Maier, B. Moritz, and T. P. Devereaux, Decrease of d-wave pairing strength in spite of the persistence of magnetic excitations in the overdoped Hubbard model. *Phys. Rev. B* **96**, 020503(R) (2017)
- [20] A. V. Balatsky, I. Vekhter, and Jian-Xin Zhu, Impurity-induced states in conventional and unconventional superconductors. *Rev. Mod. Phys.* **78**, 373 (2006).
- [21] F. Rullier-Albenque, H. Alloul, F. Balakirev, and C. Proust, Disorder, metal-insulator crossover and phase diagram in high-Tc cuprates. *EPL* **81**, 37008 (2008)
- [22] N. R. Lee-Hone, H. U. Ozdemir, V. Mishra, D. M. Broun, and P. J. Hirschfeld, Low energy phenomenology of the overdoped cuprates: Viability of the Landau-BCS paradigm. *Phys. Rev. Research* **2**, 013228 (2020)
- [23] Peter Henseler, Johann Kroha, and Boris Shapiro, Self-consistent study of Anderson localization in the Anderson-Hubbard model in two and three dimensions. *Phys. Rev. B* **78**, 235116 (2008)
- [24] T. H. Y. Nguyen, D. A. Le and A. T. Hoang, Anderson localization in the Anderson-Hubbard model with site-dependent interactions. *New J. Phys.* **24**, 053054 (2022)
- [25] Nathan Giovanni, Marcello Civelli, and Maria C. O. Aguiar, Anderson localization effects on the doped Hubbard model. *Phys. Rev. B* **103**, 245134 (2021)
- [26] P. W. Anderson, Theory of Dirty Superconductors. *J. Phys. Chem. Solids* **11**, 26 (1959).
- [27] A. A. Abrikosov and L. P. Gor'kov, On the theory of superconducting alloys. 1. The electrodynamics of alloys at absolute zero. *Zh. Eksp. Teor. Fiz.* **35**, 1558 (1958).
- [28] A. A. Abrikosov and L. P. Gor'kov, Superconducting alloys at finite temperatures, *Zh. Eksp. Teor. Fiz.* **36**, 319 (1959).
- [29] T. Cren, D. Roditchev, W. Sacks, J. Klein, J.-B. Moussy, C. Deville-Cavellin, and M. Lagues, Influence of Disorder on the Local Density of States in High- Tc Superconducting Thin Films. *Phys. Rev. Lett.* **84**, 147 (2000)
- [30] John F. Dodaro and Steven A. Kivelson, Generalization of Anderson's Theorem for Disordered Superconductors. *Phys. Rev. B* **98**, 174503 (2018)
- [31] Gaetano Campi, Alessandro Ricci, Nicola Poccia, Luisa Barba, Gianmichele Arrighetti, Manfred Burghammer, Alessandra Stella Caporale, and Antonio Bianconi, Scanning micro-x-ray diffraction unveils the distribution of oxygen chain nanoscale puddles in $\text{YBa}_2\text{Cu}_3\text{O}_{6.33}$. *Phys. Rev. B* **87**, 014517 (2013)
- [32] Alessandro Ricci, Nicola Poccia, Gaetano Campi, Francesco Coneri, Alessandra Stella Caporale, Davide Innocenti, Manfred Burghammer, Martin v. Zimmermann and Antonio Bianconi, Multiscale distribution of oxygen puddles in 1/8 doped $\text{YBa}_2\text{Cu}_3\text{O}_{6.67}$. *Scientific Reports* **3**, 2383 (2013)
- [33] Nicola Poccia *et al.* Spatially correlated incommensurate lattice modulations in an atomically thin high-temperature $\text{Bi}_{2.1}\text{Sr}_{1.9}\text{CaCu}_2\text{O}_{8+y}$ superconductor. *Phys. Rev. Materials* **4**, 114007 (2020)
- [34] J. G. Bednorz and K. A. Muller, Possible high Tc superconductivity in the $\text{Ba} - \text{La} - \text{Cu} - \text{O}$ system. *Zeitschrift für Physik B Condensed Matter* **64**, 189 (1986)
- [35] G. Campi *et al.* Inhomogeneity of charge-density-wave order and quenched disorder in a high-Tc superconductor. *Nature* **525**, 359 (2015)

- [36] Michela Fratini, Nicola Poccia, Alessandro Ricci, Gaetano Campi, Manfred Burghammer, Gabriel Aeppli and Antonio Bianconi, Scale-free structural organization of oxygen interstitials in $\text{La}_2\text{CuO}_{4+y}$. *Nature* **466**, 841 (2010)
- [37] Alessandro Ricci *et al*, Networks of superconducting nanopuddles in 1/8 doped $\text{YBa}_2\text{Cu}_3\text{O}_{6.5+y}$ controlled by thermal manipulation. *New J. Phys.* **16**, 053030 (2014)
- [38] V. Velasco and M. B. Silva Neto, Unconventional superconductivity as a quantum Kuramoto synchronization problem in random elasto-nuclear oscillator networks. *J. Phys. Commun.* **5**, 015003 (2020)
- [39] Y. Kuramoto, Self-entrainment of a population of coupled nonlinear oscillators (International Symposium on Mathematical Problems in Theoretical Physics, Lecture Notes in Physics, vol 39) ed H Araki (Berlin: Springer) 420 (1975)
- [40] Y. Kuramoto and I. Nishikawa, Statistical macrodynamics of large dynamical systems. Case of a phase transition in oscillator communities. *J. Stat. Phys.* **49**, 569 (1987)
- [41] D. Gogny, Simple separable expansions for calculating matrix elements of two-body local interactions with harmonic oscillator functions. *Nuclear Physica A* **237**(3), 399 (1975)
- [42] D. Song *et al*, Visualization of Dopant Oxygen Atoms in a $\text{Bi}_2\text{Sr}_2\text{CaCu}_2\text{O}_{8+\delta}$ Superconductor. *Adv. Funct. Mater* **29**, 1903843 (2019)
- [43] I. Zeljkovic *et al*, Nanoscale Interplay of Strain and Doping in a High-Temperature Superconductor. *Nano Letters* **14**(12), 6749 (2014)
- [44] H. Frohlich, Theory of electrical breakdown in ionic crystals. *Proc. R. Soc. Lond. A* **160**(901), 230 (1937)
- [45] T. Holstein, Studies of polaron motion: Part I. The molecular-crystal model. *Annals of Physics* **8**(3), 325 (1959)
- [46] P. Fulde and A. Ferrell, Superconductivity in a Strong Spin-Exchange Field. *Phys. Rev.* **135**, A550 (1964).
- [47] A. I. Larkin and Yu. N. Ovchinnikov, Nonuniform State of Superconductors. *Sov. Phys. JETP* **20**, 762 (1965)
- [48] Hyeonjin Doh, Matthew Song, and Hae-Young Kee, Novel Route to a Finite Center-of-Mass Momentum Pairing State for Superconductors: A Current-Driven Fulde-Ferrell-Larkin-Ovchinnikov State. *Phys. Rev. Lett.* **97**, 257001 (2006)
- [49] Roger D. Woods and David S. Saxon, Diffuse Surface Optical Model for Nucleon-Nuclei Scattering. *Phys. Rev.* **95**, 577 (1954)
- [50] D. Gogny, in Proceeding of the International Conference on Nuclear Physics, Munich, edited by J. De Boer and H. J. Mang, (North-Holland, Amsterdam, 1973), Vol. 1, p. 48.
- [51] D. Gogny, in Nuclear Self-Consistent Fields, Trieste, edited by G. Ripka and M. Porneuf (North-Holland, Amsterdam, 1975), p. 333.
- [52] J. Decharge and D. Gogny, Hartree-Fock-Bogolyubov calculations with the D1 effective interaction on spherical nuclei. *Phys. Rev. C* **21**, 1568 (1980).
- [53] C. Gonzalez-Boquera, M. Centelles, X. Vinas and L. M. Robledo, New Gogny interaction suitable for astrophysical applications. *Physics Letters B* **779**, 195 (2018)
- [54] Y. He, T. S. Nunner, P. J. Hirschfeld, and H.-P. Cheng, Local Electronic Structure of $\text{Bi}_2\text{Sr}_2\text{CaCu}_2\text{O}_8$ near Oxygen Dopants: A Window on the High-Tc Pairing Mechanism. *Phys. Rev. Lett.* **96**, 197002 (2006)
- [55] X. Zhang, H. Zhao and J. Zhu, Visualization and control of oxygen dopant ordering in a cuprate superconductor. *Materials Today Physics* **23**, 100629 (2022)
- [56] J. A. Slezak *et al*, Imaging the impact on cuprate superconductivity of varying the interatomic distances within individual crystal unit cells. *Proc. Natl. Acad. Sci. USA* **105**(9), 3203 (2008)
- [57] R. P. A. Dullens and A. V. Petukhov, Second-type disorder in colloidal crystals. *EPL* **77**, 58003 (2007)
- [58] R. Hosemann, *Z. Phys.* **128**, 1 (1950); *ibid.* 465 (1950).
- [59] R. Hosemann and A. M. Hindeleh, *J. Macromol. Sci. — Phys.* **B34**(4), 327-356 (1995).
- [60] R. Micnas, J. Ranninger, and S. Robaszkiewicz, Superconductivity in narrow-band systems with local nonretarded attractive interactions. *Rev. Mod. Phys.* **62**, 113 (1990)
- [61] P. J. H. Denteneer, R. T. Scalettar and N. Trivedi, Particle-Hole Symmetry and the Effect of Disorder on the Mott-Hubbard Insulator. *Phys. Rev. Lett.* **87**, 146401 (2001)
- [62] A. Perali, A. Bianconi, A. Lanzara and N.L. Saini, The gap amplification at a shape resonance in a superlattice of quantum stripes: A mechanism for high- T_c . *Solid State Communications* **100**(3), 181 (1996)
- [63] E. V. L. de Mello1, Description and connection between the oxygen order evolution and the superconducting transition in $\text{La}_2\text{CuO}_{4+y}$. *EPL* **98**, 57008 (2012)
- [64] Ginestra Bianconi, Superconductor-insulator transition on annealed complex networks. *Phys. Rev. E* **85**, 061113 (2012)
- [65] D. Pelc *et al*, Emergence of superconductivity in the cuprates via a universal percolation process. *Nat. Commun.* **9**, 4327 (2018)
- [66] Ginestra Bianconi, Enhancement of T_c in the superconductor-insulator phase transition on scale-free networks. *J. Stat. Mech.*, P07021 (2012)
- [67] A. Dubroka *et al*, Evidence of a precursor superconducting phase at temperatures as high as 180 K in $\text{R}(\text{Ba}_2\text{Cu}_3\text{O}_{7-\delta})$ ($R = \text{Y}, \text{Gd}, \text{Eu}$) superconducting crystals from infrared spectroscopy. *Phys. Rev. Lett.* **106**, 047006 (2011)
- [68] I. S. Burmistrov, I. V. Gornyi, and A. D. Mirlin, Enhancement of the Critical Temperature of Superconductors by Anderson Localization. *Phys. Rev. Lett.* **108**, 017002 (2012)